Far-field pressure measurements of elliptic jets discharged close to a wing

A. R. Proença[1,2], and J. L. T. Lawrence[1]

[1] Institute of Sound and Vibration Research, University of Southampton, Southampton, SO17 1BJ, UK.
[2] School of Aerospace, Transport and Manufacturing, Cranfield University, Cranfield, MK43 0AL, UK

E-mail: a.proenca@cranfield.ac.uk

Abstract. This paper presents a preliminary experimental investigation into the acoustics of two elliptical jet nozzles installed close to a wing model. Acoustic pressure data is obtained for a range of observer polar angles mounted in the far field of the jets. Three nominal jet Mach numbers, namely 0.4, 0.6 and 0.8 are studied. Results suggest that the elliptic jets surveyed provide a noise reduction of the jet-surface installation noise source. The noise reduction is maximum in the forward arc and in the order of 1 dB for the fully-corrected overall sound pressure level data. Additionally, the noise benefit exists only when the minor axis of the elliptical nozzle is mounted parallel to the wing trailing edge. It is hypothesised that the reduction in the jet plume cross-section width limits the scattering of the near pressure field by the wing trailing edge to a lower frequency range. The jet mixing noise source, however, is seen to increase with decreasing nozzle exit-plane aspect ratio. The three jet velocities surveyed suggest the consistency of the key results discussed in the paper. Investigation of the jet turbulent flow structures and jet near pressure field is under way.

1. Introduction

Engine noise is the dominant source of commercial aircraft noise. At take-off, both the mixing of the high-speed exhausted jet with the nominally stationary air and the interaction of the jet pressure field with aircraft solid surfaces (e.g., wing, high-lift devices, and fuselage) play a major role in noise generation. Thus, mitigating the jet mixing noise and the jet-surface installation noise sources is a top priority for aircraft and engine manufacturers.

Historically, passive and active noise control devices aiming at jet noise control have been studied. To be successfully used in aviation, any noise control device should offer both a significant aircraft noise reduction at either take-off or landing, and minimal thrust penalties due to increased weight or increased drag. However, this is usually not simple to obtain. On one hand, current technology rules out the use of promising active noise control systems due to aircraft performance restrictions. On the other hand, modifications to the engine nacelle and nozzle outlets are also constrained by structural and aerodynamic requirements.

Simple passive noise control mechanisms offer simple solutions, albeit limited in terms of the maximum noise reduction obtained at different flight operations. The first solutions were proposed by Westley and Lilley [1] at the same time the field of aeroacoustics was born in 1952, with the seminal work of Lighthill [2]. Some of the more successful applications to date involve

Content from this work may be used under the terms of the Creative Commons Attribution 3.0 licence. Any further distribution of this work must maintain attribution to the author(s) and the title of the work, journal citation and DOI.
Published under licence by IOP Publishing Ltd

the use of trailing edge modified nozzles, including serrations (or chevrons) and lobed nozzles. Elliptic and rectangular nozzles have also been studied, finding applications in non-conventional and supersonic aircraft.

Although it has been found that elliptic jets are not effective at reducing the jet mixing noise source of unheated, subsonic jets [3], no study has been conducted on assessing potential to jet-surface noise mitigation. In the low to moderate subsonic speeds of interest here (i.e., turbofan bypass flow), the entrainment ratio of an elliptic jet is greater than that of round and rectangular jets [4, 5, 6]. This increase in jet-ambient mixing leads to an augmentation of jet spreading rate and decreases the jet potential core length. Although the jet cross-section tends to become circular in the fully-turbulent region (i.e., two potential core lengths downstream of the nozzle exit), an oval shape is observed where the wing trailing edge is located. Thus, it is necessary to explore the installation effects propagated in installed elliptic jet configurations.

The influential work of Hussain and Husain in the early 1990s shed light into the flow instability that can be explored in the problem [7, 8, 9]. In depth investigation of instability excitation and dynamic behaviour of the coherent structures were presented. The jet cross-section deformations and complex axes switch-over were found to be dependent on the aspect ratio and initial conditions. Unfortunately, these important and fundamental investigations were performed for incompressible jets and low aspect ratios (e.g., maximum aspect ratio of 1:2), which are not representative of the investigation proposed in the paper.

Although a parametric study on different aspect ratios is relatively straight forward, a comprehensive survey into the effect of initial conditions are more demanding and difficult to control in full-scale applications. In this work, the acoustic pressure field of two elliptic nozzles are compared against a round nozzle baseline. The main focus is on the potential mitigation of the jet-surface installation (JSI) noise source.

2. Experimental Methodology

Experiments were performed in the Institute of Sound and Vibration Research, at the University of Southampton. The Doak Laboratory is an anechoic chamber, fully anechoic above 400 Hz with dimensions approximately equal to 15 m-long, 7 m-wide and 5 m-high. Two separate air supply systems allow in-flight simulations of single stream jet flows using the recently commissioned Flight Jet Rig (FJR). The primary 'core' jet flow is supplied by a high-pressure compressor-reservoir system, capable of producing a maximum inlet pressure of 20 Bar. The secondary 'flight' flow is supplied by a 1.1 pressure ratio fan. The 300 mm-diameter flight nozzle can produce flow velocities up to 100 m/s.

Temperature and pressure sensors are mounted both in the plenum (located far upstream of the nozzle exit) and along the pipework of the core and flight jet ducts. Ambient chamber properties, such as pressure, temperature and relative humidity, are also recorded. These readings are required to set the nominal jet exit velocity condition and to apply corrections to the data (e.g. atmospheric attenuation and NPR variation during the long hot-wire traverse measurements). A linear far-field microphone array is mounted close to the ceiling of the chamber. Ten microphones are used to cover polar observer angles ranging from 40° to 130°, at 10° intervals. The closest microphone, $\theta = 90°$, is located at approximately 55 jet nozzle diameters from the nozzle centreline.

A 40-mm-diameter convergent, round nozzle was used as baseline. Two elliptical nozzles were studied, both of which have the same flow area at the nozzle exit plane as the baseline. Thus, the effective diameter, $D_{\text{eff}} = 2\sqrt{R_{\text{min}}R_{\text{maj}}}$, is 40 mm for all three nozzle geometries studied. Two aspect ratios, $e = R_{\text{min}}/R_{\text{maj}}$, equal to 0.83 and 0.7, were considered. The radii along the major and minor axes of Nozzle II are 22 mm and 18.2 mm, respectively. Nozzle III had radii equal to 24 mm and 16.7 mm. Images of the anechoic chamber depicting the FJR and the far-field microphone array and the nozzles used are shown in Fig. 1.

Figure 1. Doak Laboratory (left-hand-side) and the nozzles used in the work (right-hand-side).

A 2-D (i.e., uniform chord along the spanwise direction) aerofoil was mounted next to the nozzle. This aerofoil was designed using a NACA4415 profile and had dimensions of 150 mm-chord and 600 mm-span. The aerofoil was 3-D printed in three sections and later assembled using two internal M5 threaded studs to ensure rigidity. The aerofoil trailing edge (TE) was located at $l = 3D$ and $h = 0.6D$, where l was the axial distance between the nozzle exit plane and the aerofoil TE and h was the vertical distance between the jet centreline and the aerofoil TE.

Data was acquired using high-density National Instrument modules. Each test point was recorded for 10 seconds at a sampling rate of 200,000 samples per second. Additional information about the experimental facility, instrumentation, and acquisition systems can be found in the literature [10, 11].

3. Results

The main objective of the paper is to assess whether elliptic jet nozzles demonstrate a potential to mitigate jet-surface installation noise. Thus, the following sub-section presents results for an acoustic Mach number $M = 0.6$ jet. For the close-coupled configuration studied, the JSI dominates most observer locations at low and moderate subsonic Mach numbers. Finally, in Sect. 3.2, other jet velocities are analysed to investigate the important effects on jet mixing noise of elliptic jets.

3.1. Jet-surface installation noise (JSI)

Far field spectra obtained for all ten microphones were analysed in detail. Trends were consistent for observer polar angles in the range $60° \leq \theta \leq 130°$. Using the data recorded at $\theta = 90°$, Fig. 2 illustrates the spectra of both installed jet (solid lines) and isolated jet (dashed lines) configurations. The nozzle aspect ratio 0.83 and 0.7 are shown in figures 2(a) and 2(b),

respectively. For both sub-plots, the nozzle major axis is parallel to the wing trailing edge ($\phi = 0°$ - note that this angle defines the nozzle orientation with respect to the wing, rather then an observer azimuthal angle). As expected from the literature, the isolated experiments of both elliptic jets produce consistently higher sound pressure levels than the round jet baseline. At this particular observer location, the highest difference is seen at low frequencies ($\Delta\mathrm{SPL}_{\max} \approx 2$ dB). A slightly different trend is observed for installed configurations. The low frequency hump, characteristic of the jet-surface installation source, shows a similar noise difference as in the isolated case. However, moderate- and high-frequency regions of the spectra for both round and elliptic jets are similar.

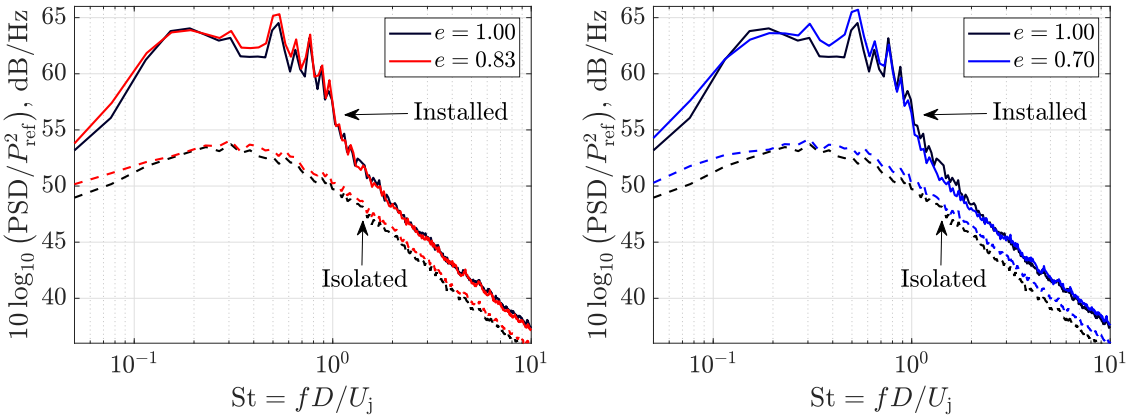

(a) aspect ratio 0.83 (b) aspect ratio 0.70

Figure 2. Sound pressure level measured at $\theta = 90°$ for isolated and installed configurations ($\phi = 0°$).

Results shown in Fig. 2 suggest that no noise benefit is obtained by the elliptic jets. One hypothesis for this observation is that although the distance between the nozzle lip to the wing surface is increased in the elliptic geometries, the higher spreading rate compared to round nozzles [5] still induce a strong interaction of the jet with the wing TE.

Setting the ellipse minor axis parallel to the wing TE means that the jet nozzle external surface is closer to the wing. Far-field results are illustrated in Fig. 3. The different lines and axes follow the same patterns as in Fig. 2. It can be seen that the JSI hump becomes slightly narrower with increasing aspect ratio. This feature also has been observed in other polar angles dominated by the JSI. The integration of the PSD levels indicate that a noise reduction of approximately -0.5 to -1 dB with respect to the round baseline is obtained for polar observer angles $\theta \geq 60°$.

The narrowing of the hump is associated with the elliptic jet cross-section. The spanwise coherent length at the wing trailing edge is, thus, reduced in comparison to the round jet. This result is also similar when short wing chords, or flap only configurations are considered [12]. Further investigation is being conducted to clarify this hypothesis.

In Fig. 4, results obtained at $\theta = 130°$ are displayed. Figure 4(a) shows data at $\phi = 0°$, and Fig. 4(b) at $\phi = 90°$. Despite similar trends as figures 2 and 3, a secondary, small hump starts to develop around Strouhal number $\mathrm{St} \approx 5$ at this polar angle. As this high-frequency trend 1) develops consistently with decreasing aspect ratio, and 2) propagates only to the high forward arc angles, it is believed that this phenomenon is due to the passage of waves through the small gap between the nozzle and wing surfaces. Nonetheless, the low PSD values compared to the low-frequency content, and atmospheric attenuation reduce the importance of this feature to practical applications.

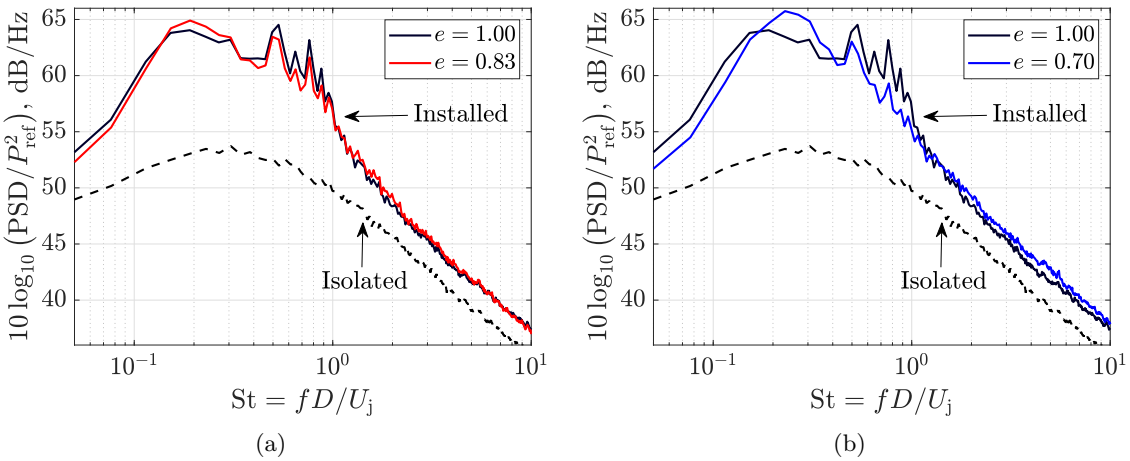

Figure 3. Sound pressure level measured at $\theta = 90°$ for isolated and installed configurations ($\phi = 90°$).

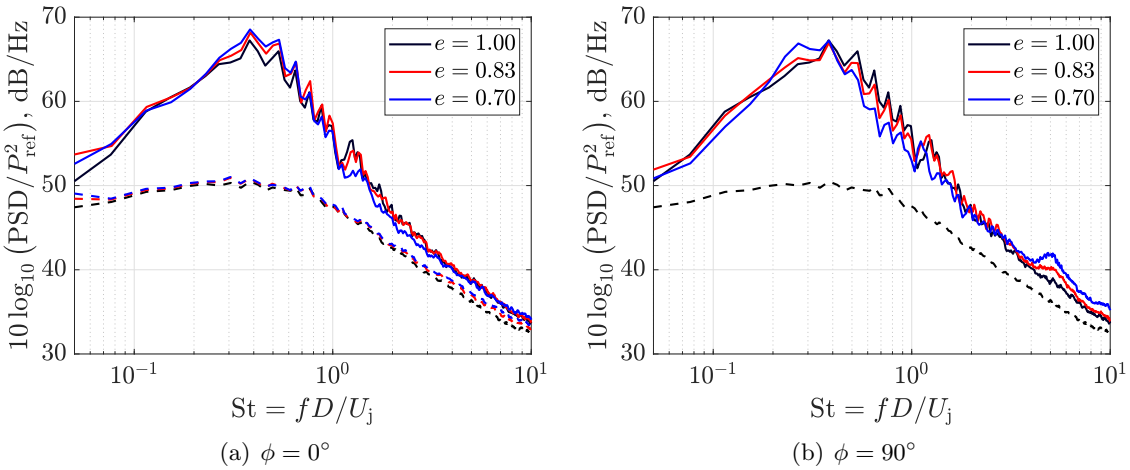

Figure 4. Sound pressure level measured at $\theta = 130°$ for isolated and installed configurations.

Although the $\phi = 90°$ showed some potential to JSI noise reduction, the narrowing of the hump is overshadowed by the high peak level at $0.2 \leq \mathrm{St} \leq 0.3$. To alleviate this, other passive noise control mechanisms can be used in conjunction with elliptic nozzles (e.g., chevrons). Ideally, to obtain similar noise reduction in dB levels, any additional passive flow control mechanism would be less intrusive in the elliptic jet compared to a round jet counter-part.

3.2. Jets dominated by mixing noise

The results presented in the previous sub-section were substantially different at low polar angles (e.g., $\theta = 40°$). This prompted an investigation into other jet velocities and isolated jets, in which the jet mixing noise component either dominates the JSI noise source or at least plays an important role in the total noise generated.

Figure 5 shows the power spectral density measured for installed and isolated configurations at $\theta = 40°$. The elliptic nozzle angles of each sub-plot and the lines for all three nozzles are indicated in the Figure.

First of all, for installed configurations, results display very different, if not the opposite behaviour observed at higher polar angles. The major axis orientation (Fig. 5(a)) of elliptic jets

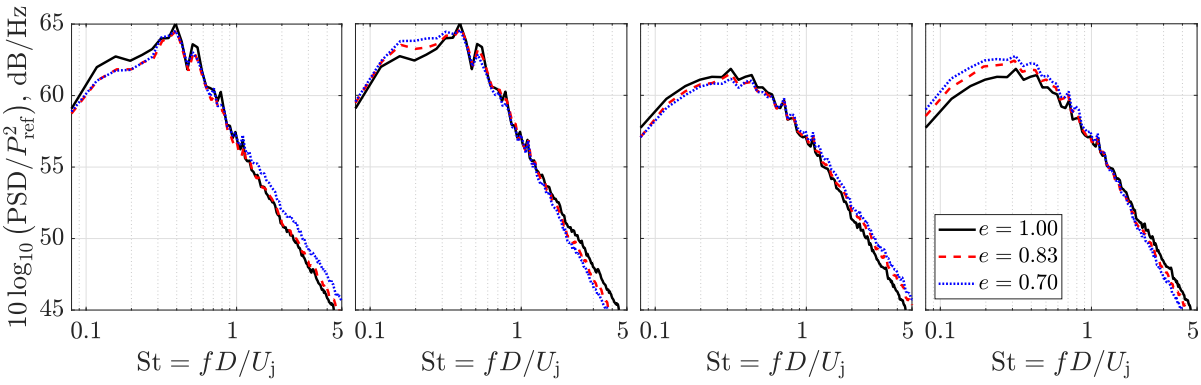

(a) Installed, $\phi = 0°$ (b) Installed, $\phi = 90°$ (c) Isolated, $\phi = 0°$ (d) Isolated, $\phi = 90°$

Figure 5. Sound pressure level measured at $\theta = 40°$ for isolated (LHS) and installed (RHS) configurations. Ellipse orientation indicated in each sub-figure.

produced lower PSD levels at low-frequency compared to the round baseline, whilst the minor axis setup increased the far-field noise. This behaviour is difficult to explain. However, the plots shown in figures 5(c) and 5(d) reveal that the isolated and installed configurations produce similar noise levels, especially for $\phi = 90°$. Thus, it is confirmed that the counter-intuitive trend after studying the other polar angles is due to jet mixing noise, rather than the JSI noise source.

Finally, the other jet velocities carried out during the experiments were studied. To present the key results of this investigation in the paper, Fig. 6 shows the sound pressure level (SPL) of the round and two elliptic nozzles measured at acoustic Mach numbers $M = 0.4$ and $M = 0.8$, and at observer polar angle $\theta = 90°$. Sound pressure level measured at $M = 0.6$ for the round jet (data from Fig. 2) is also displayed for reference.

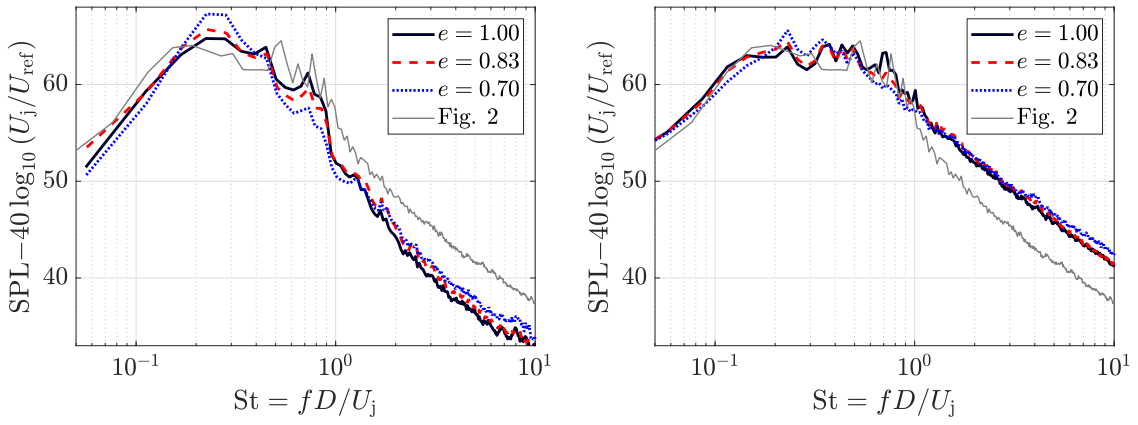

(a) $M_{\mathrm{j}} = 0.4$ (b) $M_{\mathrm{j}} = 0.8$

Figure 6. Sound pressure level measured at $\theta = 90°$ for round and elliptic jets ($\phi = 90°$)

To compare the two different jet velocities in each sub-plot, the SPL data was corrected by the 4^{th} power of the jet exit velocity. Although this correction factor should work for the low frequencies dominated by the JSI hump, it certainly produces the disagreement seen at high-frequencies from around St $= 1$. These higher frequencies are dominated by the jet mixing noise and should scale with U_{j}^7 (in a dB/Hz plot, at $\theta = 90°$). Nonetheless, results presented in Fig. 6 confirm that: 1) the JSI noise source of elliptic jets scale with jet exit velocity in the

same manner as round nozzles, and 2) the hump narrowing phenomenon are indeed observed at low and moderate Mach numbers (JSI dominates), but not for high-subsonic speeds (jet mixing noise dominates).

4. Conclusions

This paper presented an experimental survey on the far pressure field on elliptic jets. A round baseline jet and two elliptic jets were investigated. The nominal jet Mach numbers were set at 0.4, 0.6 and 0.8. Acoustic data was recorded at ten observer polar angles.

The analysis presented in the paper suggest that the results for isolated jet configurations are in agreement with previous works. At all observer locations, elliptic jets produced similar or higher overall sound pressure levels in the jet far field. This is seen to be true also for installed configurations in which the ellipse major axis is parallel to the wing trailing edge.

On the other hand, noise reductions of up to 1 dB overall were observed for installed configurations with the ellipse minor axis aligned with the wing TE. The maximum benefit is seen in the jet forward arc, where the jet-surface installation effects dominate the jet mixing noise source. The spectra displayed in the paper indicate that the well-known 'hump' signature of the JSI noise source reduces its width with decreasing nozzle aspect ratio.

Although the major axis alignment increases the distance between the nozzle lipline and the plate surface, the minor-axis plane contains most of the jet entrainment process [4, 5]. Thus, the interaction between the jet rotational flow-field and wing structure is still important in that orientation. Mounting the minor axis parallel to the wing TE discharges the jet closely to the wing. However, compared to round jets, the width of the jet plume is reduced at the wing TE location. This is believed to induce a lower coherence along the span of the TE.

Other passive noise control devices can be used in conjunction with elliptic jet nozzles. For example, it is hypothesised that a combination of elliptic nozzles with less intrusive chevrons could provide similar benefits to noise mitigation compared to current serrated round nozzles with higher penetration angles. Other future study would feature the analysis of the jet flow-field, near-field, and wall-pressure fields of elliptic jets with practicable aspect ratios. One interesting phenomenon that could be explored is the switch in orientation of the major and minor axes downstream of the nozzle exit caused by the auto-induction deformation of the elliptic ring vortices at the nozzle exit [13, 14]. The axis-switching location has been shown to vary linearly with aspect ratio, taking place at $x/D_\mathrm{j} \approx 2$ for a $e = 0.5$ elliptic jet. Thus, further studies on the effects of wing TE location on the results discussed above are recommended.

Acknowledgments

This research has received funding from the European Union's Horizon 2020 research and innovation programme, grant No. 769 350 (ARTEM project, https://cordis.europa.eu/project/id/769350).

References

[1] R. Westley and G. M. Lilley. An investigation of the noise from a small jet and methods for its reduction. College of Aeronautics - Cranfield Report 53, 1952.

[2] M. J. Lighthill. On sound generated aerodynamically. i. general theory. *Proceedings of the Royal Society of London A: Mathematical, Physical and Engineering Sciences*, 211(1107): 564–587, 1952. ISSN 0080-4630. doi: https://doi.org/10.1098/rspa.1952.0060.

[3] Xavier Tesson, Benoit Petitjean, and Dennis McLaughlin. *Experiments on the Noise Produced by High Speed Jets with Elliptic Nozzles*. 2005. doi: 10.2514/6.2005-211. URL `https://arc.aiaa.org/doi/abs/10.2514/6.2005-211`.

[4] Chih-Ming Ho and Ephraim Gutmark. Vortex induction and mass entrainment in a small-aspect-ratio elliptic jet. *Journal of Fluid Mechanics*, 179:383–405, 1987. doi: 10.1017/S0022112087001587.

[5] K. B. M. Q. Zaman. Spreading characteristics of compressible jets from nozzles of various geometries. *Journal of Fluid Mechanics*, 383:197–228, 1999. doi: 10.1017/S0022112099003833.

[6] K Knowles and A J Saddington. A review of jet mixing enhancement for aircraft propulsion applications. *Proceedings of the Institution of Mechanical Engineers, Part G: Journal of Aerospace Engineering*, 220(2):103–127, 2006. doi: 10.1243/09544100G01605. URL `https://doi.org/10.1243/09544100G01605`.

[7] Fazle Hussain and Hyder S. Husain. Elliptic jets. part 1. characteristics of unexcited and excited jets. *Journal of Fluid Mechanics*, 208:257–320, 1989. doi: 10.1017/S0022112089002843.

[8] Hyder S. Husain and Fazle Hussain. Elliptic jets. part 2. dynamics of coherent structures: pairing. *Journal of Fluid Mechanics*, 233:439–482, 1991. doi: 10.1017/S0022112091000551.

[9] Hyder S. Husain and Fazle Hussain. Elliptic jets. part 3. dynamics of preferred mode coherent structure. *Journal of Fluid Mechanics*, 248:315–361, 1993. doi: 10.1017/S0022112093000795.

[10] Anderson Proença, Jack Lawrence, and Rod Self. Experimental investigation into the turbulence flowfield of in-flight round jets. *AIAA Journal*, 58(8):3339–3350, 2020. doi: 10.2514/1.J059035. URL `https://doi.org/10.2514/1.J059035`.

[11] Anderson Proença. *Aeroacoustics of isolated and installed jets under static and in-flight conditions*. PhD thesis, University of Southampton, March 2018. URL `https://eprints.soton.ac.uk/426880/`.

[12] J. G. Shearin. Investigation of jet-installation noise sources under static conditions. Unknown, August 1983.

[13] H.E. Fiedler and H.-H. Fernholz. On management and control of turbulent shear flows. *Progress in Aerospace Sciences*, 27(4):305–387, 1990. ISSN 0376-0421. doi: https://doi.org/10.1016/0376-0421(90)90002-2. URL `https://www.sciencedirect.com/science/article/pii/0376042190900022`.

[14] Sang-Joon Lee and Seung-Jo Baek. The effect of aspect ratio on the near-field turbulent structure of elliptic jets. *Flow Measurement and Instrumentation*, 5(3):170–180, 1994. ISSN 0955-5986. doi: https://doi.org/10.1016/0955-5986(94)90016-7. URL `https://www.sciencedirect.com/science/article/pii/0955598694900167`.

https://dspace.org/

Far-field pressure measurements of elliptic jets discharged close to a wing

Ramos Proenca, Anderson; Lawrence, Jack L. T.

2022-02-15
IOP Publishing
https://doi.org/10.1088/1757-899X/1226/1/012048
Proenca AR, Lawrence JLT. (2022) Far-field pressure measurements of elliptic jets discharged close to a wing. In: International Conference on Innovation in Aviation & Space to the Satisfaction of the European Citizens (11th EASN 2021), 1-3 September 2021, Virtual event.

Downloaded from a DSpace repository. https://dspace.org/